NeuroImage 324 (2025) 121621

Contents lists available at ScienceDirect

NeuroImage

journal homepage: www.elsevier.com/locate/ynimg

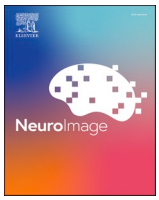

Anatomical characterization of premotor-motor connectivity in humans by paired intraoperative direct cortical stimulation

Luigi Cattaneo [a,b,*], Sonia Nunes [c], Davide Giampiccolo [d,e], Valeria Di Caro [c], Federica Basaldella [f], Andrea Badari [f], Marco Tagliaferri [a], Giovanna Squintani [f], Francesco Sala [c]

[a] Center for Mind/Brain Sciences (CIMeC) – University of Trento, Italy
[b] Center for Medical Sciences (CISMed) – University of Trento, Italy
[c] Section of Neurosurgery, Department of Neurosciences, Biomedicine and Movement Sciences, University of Verona, Verona, Italy
[d] Department of Epilepsy, UCL Queen Square Institute of Neurology, University College London, London, UK
[e] Victor Horsley Department of Neurosurgery, National Hospital for Neurology and Neurosurgery, Queen Square, London, UK
[f] Azienda ospedaliero-universitaria integrata di Verona, Italy

ARTICLE INFO

Keywords:
Premotor
Voluntary movements
U-fibers
Motor cortex
Grasping
Reaching
Sensorimotor transformation
Cortico-cortical
Corticospinal
Pyramidal
motor

ABSTRACT

The human motor cortex represents the major source of corticospinal output and receives input from a constellation of sensorimotor regions in the surrounding cerebral cortex and subcortical regions. Here we tested cortico-cortical connections by means of direct cortical stimulation in intraoperative settings. We used short trains of 3 pulses (0.2 ms duration, 2 ms ISI) as test stimuli to the motor cortex and as conditioning stimuli to the premotor cortex in 14 human patients undergoing brain surgery for tumour resection under general anaesthesia with intraoperative neurophysiological monitoring. We observed that short-latency inhibitory conditioning effects clustered in two distinct regions within the precentral sulcus: a dorsal premotor cluster was centred around the mean coordinates (MNI) of x=±21.23; y=-4.52; z = 69.67 and a ventral premotor cluster around the x=±51.81; y = 2.03; z = 45.32 coordinates. A third cluster, with excitatory effects was found along the convexity of the superior frontal gyrus (SFG), around the mean coordinates of x=±15.87; y = 9.84; z = 64.34. The earliest effective ISIs were: 4 ms for the dorsal and ventral precentral clusters, compatibly with direct cortico-cortical connections. The SFG cluster exerted conditioning effect on M1 at shortest ISI of 8 ms, compatible with either direct or indirect connections to M1. We show that intraoperative neurophysiology can assess premotor-motor connections with a Conditioning-Test stimulus technique. The two inhibitory precentral foci are compatible with human equivalents of dorsal and ventral premotor cortices in non-human primates. The SFG cluster may be related to flexible control of upper limb movements.

1. Introduction

The premotor cortex (PM) lies immediately rostral to the primary motor cortex (M1) and plays a pivotal role in the cortical motor system of primates (Rizzolatti et al., 2014). The PM is the main recipient of highly pre-processed sensory information that is built up in the parietal cortex, but receives also information from the prefrontal cortex (Rizzolatti and Luppino, 2001). Therefore, it receives the relevant sensory information to perform goal-directed actions together with the executive inputs that allow for action flexibility (Cisek and Kalaska, 2010). In addition to this, the medial portion of the PM contains a machinery for temporal estimation (Casini and Vidal, 2011) and is the target of motivated, value-based decisions coming from the medial prefrontal system (Coull et al., 2016). Overall, the PM is provided with information to arbitrate motor content (what to do), manner (how to do it), timing (when to do it) and motivation (if it is worth doing it). The PM has predominant motor properties as it shows neural activity that correlates with and decodes overt actions - and it can induce overt movements or their interruption when stimulated. The PM hosts complex movement representations or archetypes, involving several joints and different, sometimes bilateral, effectors (Graziano, 2016).

According to influent non-human primate models (Rizzolatti et al.,

* Corresponding author.
E-mail address: luigi.cattaneo@unitn.it (L. Cattaneo).

https://doi.org/10.1016/j.neuroimage.2025.121621
Received 24 May 2025; Received in revised form 8 November 2025; Accepted 25 November 2025
Available online 26 November 2025

2014), the premotor region is spatially parcelled into separate modules that show local specialization of function. We recognize at least 3 main functional units (Caminiti et al., 2015). A first, ventral PM region (PMv) receives mostly spatially-invariant, object-centred information from the parietal cortex about object features and that controls mainly upper-limb and orofacial movements. A second, dorsal PM region (PMd) that receives spatially-sensitive information from the personal and peripersonal spaces, and controls mainly proximal and axial movements. A third, medial premotor region (including the supplementary motor area, SMA) with limited access to sensory information but massive input from the medial prefrontal system, where motivated, value-based goals are represented that is involved in initiation/stopping and internal clocking of actions (Coull et al., 2016).

It is still a matter of discussion whether the mechanism of communication between PM and the spinal cord, to produce movements is based on direct PMC-spinal connections or rather by indirect connections through PM-M1 and the M1-spinal cord connectivity (Lemon, 2019). It is likely that both mechanisms coexist, but the respective contribution of the two output modalities of PM to actual behaviour is unclear. It has been argued that, compared with corticospinal projections from M1, those from PM play only a minor role in controlling hand movements, mostly terminating in the upper cervical spinal segments and only to a lesser extent directly to the caudal segments of the cervical enlargement, where the motor nuclei innervating the hand muscles are located (Dum and Strick, 2005).However, some effects on hand muscle motoneurons may be exerted by PM indirectly through C3–C4 propriospinal neurons located in the upper cervical cord (Borra et al., 2010; Isa et al., 2013). On the contrary, human and non-human primate works seem to highlight a main role of cortico-M1 connections in transforming specific information on planned actions into a motor act (Bäumer et al., 2009a; Shimazu et al., 2004). In macaques, although both PMd and PMv contribute some corticospinal projections, they also exert their influence through cortico-cortical projections to M1, which in turn is the major source of the corticospinal tract, with well-established, powerful, and direct actions on spinal motoneurons (Shimazu et al. 2004; Dum and Strick 2005; Lemon, 2008). Also in humans PM-M1 interactions are likely to be the main pathway of PMC's access to the spinal cord, given the scarcity of corticospinal projections from the PM (Fornia et al., 2018) and the powerful PMC-M1 functional connectivity that non-invasive brain stimulation (NIBS) studies have highlighted (Koch, 2020).

One potential application of the present work regards the increasingly popular use of paired TMS pulses to build associative plasticity in brain circuits (Casarotto et al., 2023; Di Luzio et al., 2024; Pötter-Nerger et al., 2009). The current results could provide supporting information for such procedures regarding both anatomy and timing of the stimuli.

Summing up, understanding PM-M1 connectivity is critical for understanding the cortical motor system. This should be anatomically constrained, because PM-M1 connections arising from different subregions are likely to carry discrete, specific motor plans such as hand-object interactions (ventral), spatially-oriented behaviour (dorsal) and motivated internally-timed behaviour (medial). In humans cortico-cortical connectivity may be tested non-invasively by means of dual coil-transcranial magnetic stimulation (TMS) techniques. These are based on a well-established conditioning-test stimulus paradigm in which a suprathreshold test stimulus is delivered to M1, thus eliciting a motor response that is recorded in the form of a Motor Evoked Potential (MEP). If the test stimulus is preceded by a conditioning stimulus applied to a premotor cortical region that does not have significant access to the spinal cord, but that does have direct connectivity to M1, then the amplitude of the MEPs can change (Cattaneo and Barchiesi, 2011). Notably, the change in MEP amplitude is informative of effective connectivity, because the neural information can be read in the temporal and spatial pattern of MEP modulation (Lafleur et al., 2016). Current neurophysiological findings using dual coil TMS have shown that intra-hemispheric PM-M1 connections convey several types of motor plans to M1, ranging from object-relevant information for grasping (Davare et al., 2009; Maule et al., 2015), to action initiation/selection (Koch and Rothwell, 2009; Parmigiani et al., 2018, 2015). The TMS dual-coil protocols that are used for non-invasive measurement of cortico-cortical connections are sub-optimal due to the size of the stimulating coils, that does not allow for the assessment of nearby regions. While this limitation does not apply to inter-hemispheric (Ferbert et al., 1992) or cerebello-cortical (Ugawa et al., 1995) protocols, it affects particularly intra-hemispheric protocols, where the premotor and parietal regions at the origin of cortico-cortical connections to M1 are very close to the primary motor cortex (Groppa et al., 2012; Hehl et al., 2024a; Parmigiani et al., 2015, 2018; Shields et al., 2016).

Invasive brain stimulation is the mainstay of the clinical procedures of intraoperative neurophysiological monitoring (IONM), which has a fundamental clinical role in aiding safe neurosurgical resection (Giampiccolo et al., 2022). Very recently, intraoperative dual stimulation techniques inspired by the non-invasive protocols, have been proposed to monitor the integrity of association and projection fibers during surgery (Sala et al., 2021). In addition to their potential clinical utility, intraoperative paired-pulse techniques offer potential high spatial resolution information on the anatomy of premotor-M1 connections. For example, a recent work exploiting this technique, confirmed the existence in humans of parietal-M1 connections with considerable spatial accuracy (Cattaneo et al., 2020). In the present work we aim at describing the spatial and temporal pattern of PM-M1 connections, by means of invasive stimulation used for IONM.

2. Patients and methods

14 patients, aged 24–72 years, undergoing elective oncological neurosurgery with tumors located in the frontal and parietal regions were recruited after providing informed consent to the procedure, which had been approved by the Review Board for Ethics Committee for Clinical Trials (CESC) of the University of Verona (Prog. 255CET) and carried out in accordance with ethical standards of the Declaration of Helsinki (World Medical Association, 2013). Written informed consent was obtained from all patients before the study began. Cumulative lesion volumes are illustrated in Fig. 1. Demographics and anatomo-clinical data are reported in Table 1. None of the experimental procedures interfered with the clinical management of the patient, and experimental intraoperative neurophysiology was performed only in patients requiring clinical intraoperative monitoring of the motor system. Patients were evaluated during general anaesthesia, after opening of the skull and dura, by means of direct electrical stimulation of the cortex, with CS/TS dual-pulse paradigm.

2.1. Anesthesia and clinical intraoperative monitoring

The Total Intravenous Anesthesia (TIVA) protocol was used, consisting of a continuous infusion of Propofol (100–150 μg/kg/min) and Fentanyl (1μg/kg/min) whilst avoiding any boluses. Short acting relaxants were administered for intubation purposes only and then avoided. Halogenated anaesthetic agents were not administered. The current anaesthetic protocol allows the electrical activation of the corticospinal tract (Giampiccolo et al., 2022) and is appropriate for the assessment of short-latency brain connectivity (Cattaneo et al., 2020). Neurophysiological monitoring was performed on the ISIS- Expert Inomed System (Inomed Medizintechnik GmbH, Emmendingen, Germany). Neurophysiological baselines traces were acquired prior to dura opening. These modalities comprised of continuous electroencephalography (EEG), electrocorticography (ECoG), recording of free-running electromyography (EMG), Transcranial Motor Evoked Potentials (TES-MEPS) and Somatosensory Evoked Potentials (SEPS) were required for the clinical evaluation of neurophysiological signals. EMG recordings for clinical monitoring were conducted on a standard set of muscles: *orbicularis oris*, the *abductor pollicis brevis* (APB), the *extensor carpi radialis*

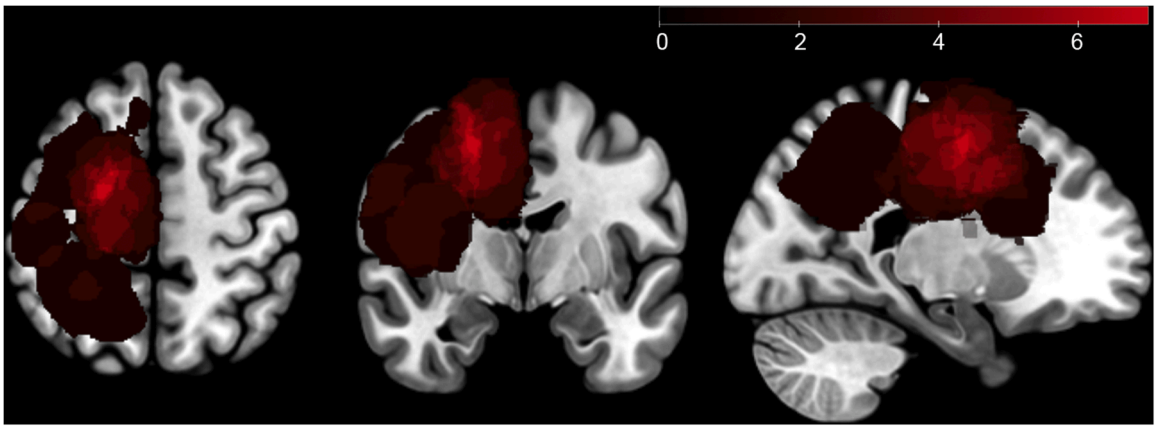

Fig. 1. lesion overlap of the 14 patients. Note that all lesions have been flipped to the left hemisphere for comparison.

Table 1
Demographic and clinical data of patients. classification and grading reported according to the WHO classification which was the reference at the time of surgery (WHO 2016).

Patient ID	Age	Gender	Affected hemisphere	Lesion localization	Lesion volume (cm3)	Lesion histology (WHO classification)
1	77	M	Right	TP	11.5	Glioblastoma (IV)
2	54	M	Right	T	101.96	Astrocytoma (III)
3	61	M	Left	F	58.18	Oligodendroglioma (III)
4	71	M	Left	P	10.17	Metastasis
5	36	F	Right	P	74.33	Glioblastoma (IV)
6	52	M	Left	F	26.54	Glioblastoma (IV)
7	54	M	Right	FP	93.33	Meningioma
8	62	F	Left	F	3.28	Metastasis
9	60	M	Right	P	1.6	Cavernoma
10	65	F	Left	FT	9.12	Glioblastoma (III)
11	54	F	Left	F	27.52	Metastasis
12	43	M	Left	F	45.4	Oligodendroglioma (III)
13	39	F	Right	F	35.2	Glioblastoma (III)
14	58	F	Left	F	58.4	Glioblastoma (III)

Abbreviations: *P* = Parietal; *F* = frontal; *T*= Temporal; FT= fronto-temporal; TP= temporo-parietal; FP = fronto-parietal.

(ECD), the *biceps*, the *abductor hallucis* and the *tibialis anterior* muscles contralateral to the stimulated hemisphere. During general anaesthesia, once the dura was open, we applied a conditioning/test stimulus (CS/TS) dual-pulse paradigm in conjunction with routine neurophysiological monitoring.

2.2. Conditioned paradigm using cortical direct electrical stimulation (DES)

For the purposes of the experimental recordings, all parameters were optimized for recording from the ECD muscle. EMG recordings were performed in a belly-tendon montage, by means of subcutaneous needle monopolar electrodes (Ambu® Neuroline Subdermal, Ambu, Copenhagen, Denmark) from the ECD muscle. The analogue signal was amplified 1000x and digitized at a sampling frequency of 10 KHz. The EMG traces were then band-pass filtered in the 5Hz-5KHz range. Cortical DES was performed using two separate electrode strips placed directly on the cortical surface to deliver the TStim over M1 and the CStim over the premotor region. The strips were left in position throughout the recordings. Each strip had either 6 or 8 electrode contacts round in shape and 8 mm in radius, assembled linearly, at a distance of 10 mm between the center of adjacent leads. Stimulation was delivered in bipolar pairs between 2 adjacent electrodes, in short trains of 3 square pulses, with 0.2 ms in duration and 2 ms inter-stimulus intervals. The TStim intensity was optimised to obtain a MEP of 500 uV in the target muscle and the CStim intensity was set at the same intensity. TStim was delivered over the hand-related M1 whilst the CStim was delivered over a region PMv or PMd depending on the location of craniotomy. Stimuli were delivered in blocks of 16 trials of either CStim alone, TStim alone or CStim+TStim. In the paired stimulation blocks, the Inter-stimulus interval (ISI) was calculated between the start of the CStim train and the start of the TStim train varied systematically between the values of 4.6–8–12 ms. Note that the earliest ISI possible was 4.6 ms because the recording apparatus did not allow superimposition of the CStim train and the TStim train, therefore the earliest ISI possible corresponded to the actual duration of the CStim train. For simplicity, we will refer from now on to the 4.6 ms ISI as the "4 ms ISI". The different ISIs were fixed within each block, but in a randomized order between blocks. Therefore, for each CStim electrode that was explored, we perfomed 5 blocks of 16 stimuli each: 1 CStim alone block (not analyzed) and 4 CStim+TStim blocks, one for each of the 4 ISIs. The single block of CStim alone trials was applied only once at the beginning of the experiment to ascertain that CStim alone did not evoke any MEP. Lead pairs in which CStim alone evoked MEPs in the upper limb were excluded from further recordings. A total of 4 TStim alone blocks were delivered interleaved with CStim+TStim blocks. Summing up, in every single patient we collected 16 MEPs for each electrode and for each ISI, and a total of $16 \times 4 = 64$ MEPs from TStim alone. Electrode strip placement was highly dependent on the surgical procedure, i.e. depending on the site and size of craniotomy, however, the possibility to slide the strip under the dura, under the intact skull (Cattaneo2020) allowed for exploration of a larger cortical area radially extending from the craniotomy, the size of which was strictly determined on independent clinical bases, relative to the size of the tumour and the surgical approach. The number of electrodes that were hidden from view ranged from 0 to 3 in each recording placement. The location of the "hidden" electrodes was estimated on the 3D rendering of the

brain surface in native space base don the trajectory of the visible electrodes. The a priori target cortical region for CStim was the premotor region (Brodmann's area 6 - BA6) as defined in the Julich atlas (Amunts et al., 2020) by the cortical parcels 6d and 6v. Exploration of the ventralmost portion of BA6 was sparse, due to the distance from hand-M1. The overall duration of the recording procedure was variable surgical time but ranged generally in the 20–30 min interval.

2.3. Data analysis: MEPs

Peak-peak MEP amplitudes were the main experimental variable, as expressions of excitability of the M1 corticospinal system (Cattaneo, 2017). All MEPs were also visually inspected to exclude noisy trials (e.g., with overlapping activity from the electrosurgical unit). Overall, <2 % of trials were discarded, but since extra trials were always collected, the numerosity of 16 trials per block was preserved in all conditions. The main data analysis was aimed at demonstrating a significant difference between MEP amplitudes at TStim alone compared to MEP amplitudes at CStim+TStim. We therefore compared the MEP amplitudes from the blocks with CStim+TStim to the MEP amplitudes of all 4 blocks with TStim alone, by means of *t*-tests for independent samples. Note that given the long-range temporal fluctuations of MEPs during surgery, in order to obtain a reliable baseline, we collected the TStim blocks scattered along the whole duration of the experimental recordings. Given the univariate approach, we applied to every single patient, the Bonferroni-Holmes correction for multiple comparisons. The number of comparisons changed between patients, according to how many points had been tested, therefore ranging between 12 (3 points*4 ISIs) to 24 (6 points*4 ISIs) multiple comparisons.

2.4. Data analysis: brain mapping

Lesion volumes were generated using a semiautomatic cluster segmentation approach with the ITK-SNAP software (Yushkevich et al., 2006), (available at www.itksnap.org) and flipped the left hemisphere for direct comparison. (See Fig. 1). The anatomical localization of the CS electrodes was first pointed on the native brain space by means of the intraoperative stereotaxic neuronavigator's probe and then normalised to the MNI space using the FLIRT module in the FSL software (Woolrich et al., 2009). In case of strips partially under the dura, the position of the occluded electrodes was reconstructed on the basis of the visible electrodes, being the strip a linear array with electrodes at regular distances. Once each electrode position was reconstructed, the individual brains were normalized to the MNI space. Bipolar stimulation is more superficial and focal than monopolar stimulation, however it poses the problem of the actual site of stimulation. Anodal stimulation elicits action potentials preferentially in axons that are perpendicular to the stimulating dipole, conversely, in the tissue under the cathode, axons that are parallel to the stimulating dipole are depolarized preferentially (Hanajima et al., 2002; Iles, 2005; Manola et al., 2007; Yamada et al., 2021). The result is that at least theoretically, anodal current excites preferentially the axon of pyramidal cells on the crown of the gyri and the interneurons on the bank of the sulci; vice-versa, cathodal currents excite preferentially the axons of pyramidal cells on the bank of the sulci and the interneurons on the crown of the gyri. In our setup, however, it is probably of limited interest to distinguish between the two electrodes, for two reasons. First, the anode and cathode are in very close spatial proximity (10 mm from the electrode centres, 5 mm from the electrode margins); second, the complex geometry of the cortical folds in the realistic frontal cortex makes it that under every electrode there always seem to be a variable proportion of cortex that is parallel or perpendicular to the electrodes. For the above reasons, we decided to consider, as the putative site of stimulation, the midpoint between the two electrodes. To produce population-level data, we could not use the single spots because Cstim targets from a single subject do not represent independent data points. This part of the analysis was carried out with a custom-written Python script, using the Nilearn (Machine learning for NeuroImaging in Python) toolbox (Abraham et al., 2014). To obtain spatial information at the group level, we first analysed each subject individually, by considering only the effective CStim coordinates. We projected these coordinates onto the surface of the pial-left surface template from FreeSurfer and interpolated an area around those spots with a 10 mm margin from each coordinate. All individual active surfaces were then superimposed to produce a heatmap of the density of overlap of individual maps, and a local maximum was identified. Finally, the topography of local maxima for each post-TMS effect was compared with the parcellation of the premotor and parietal cortices of the Julich brain atlas (Amunts et al., 2020). This procedure was carried out separately for the effective CStim spots that produced excitatory effects and for those that produced inhibitory effects.

3. Results

None of the patients suffered from immediate nor delayed undesired effects of the procedure, which was performed as an integrated part of clinical IONM of the corticospinal tract. Individual electrode strip positions are shown in Fig. 2, while the cumulative electrode coverage of the cortex is shown in Fig. 3A and the cumulative effective conditioning electrodes are shown in Fig. 3B The results of the overlap density maps are shown in Fig. 4. Table 2 indicates the MNI coordinates of each cathode in individual subjects. MEP amplitude analysis was performed on the Extensor digitorum communis muscle, as this was the muscle that has been recorded systematically in all patients in the clinical montage and, in addition, is the muscle showing more stable MEP amplitude across. The mean amplitude of EDC test MEPs was 429 uV ± 20 (SEM) obtained with a mean intensity stimulation intensity of 16.1 (± 5.2) mA. Analysis of conditioned MEP amplitude compared to test MEPs showed a significant effect in 9/14 patients. Fig. 5 shows the mean MEP amplitudes in each condition in each patient. The individual numerical values are reported as Supplementary material in **Supplementary Table 1**. The effects were predominantly inhibitory or predominantly excitatory, according to the location. We observed that the cathodes with significant effects were clustered into 3 large groups: one along the convexity of the superior frontal gyrus (SFG) and 2 along the precentral sulcus, of which one occupied the dorsal precentral branch (dPreCS) and the other occupied the ventral precentral branch (vPreCS). The local maxima of the overlap density maps (Fig. 4) in MNI space are the following: inhibitory vPreCS cluster: $x=-51.81,\ y=2.03,\ z=45.32$; inhibitory dPreCS cluster: $x=-21.23,\ y=-4.52,\ z=69.67$; excitatory SFG cluster: $x=-15.87,\ y=9.84,\ z=64.34$. Due to small sample numerosity, an inter-side comparison was not possible in quantitative terms, but qualitative assessment showed that electrodes in each cluster were distributed evenly between both hemispheres (see Table 2). The local maxima coordinates were then mapped onto the Julich atlas of cortical anatomy (Amunts et al., 2020). The inhibitory vPreCS cluster corresponded to the border between area 6v3 (probabilistic assignment: 0.43) and area 6v2 (probabilistic assignment: 0.30). The inhibitory dPreCS cluster corresponded with comparable probabilities to area 6v1 (probabilistic assignment: 0.56) and area 6v2 (probabilistic assignment: 0.44). The excitatory SFG cluster corresponded to anterior area 6d2 (probabilistic assignment: 0.59) and only with a negligible probability to 6d3 (probabilistic assignment: 0.03). We extracted the minimum and average effective ISI for each of the 3 clusters. This measure however should be interpreted with the caveat that we explored ISIs changing every 4 ms, and therefore the temporal resolution of such data is coarse. The inhibitory dPreCS cluster had a minimum effective ISI ranging 4–8 ms and average earliest effective ISI of 5.3 ms. The excitatory SFG cluster had a minimum effective ISI ranging between 8 and 12 ms and average earliest effective ISI of 9.7 ms. The inhibitory vPreCS cluster had a minimum ISI ranging between 4 and 8 ms and average earliest effective ISI of 5.3 ms.

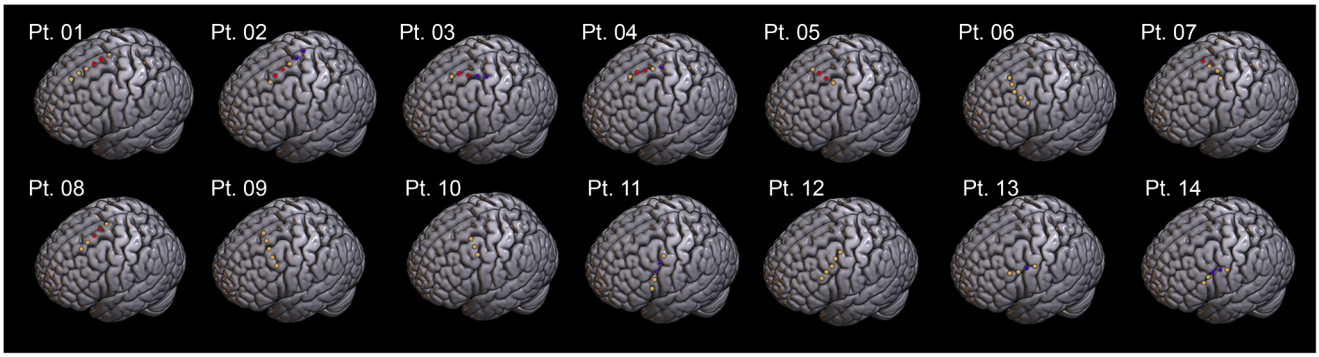

Fig. 2. individual localization of strip cathode electrodes on a MN1 152 standard brain.

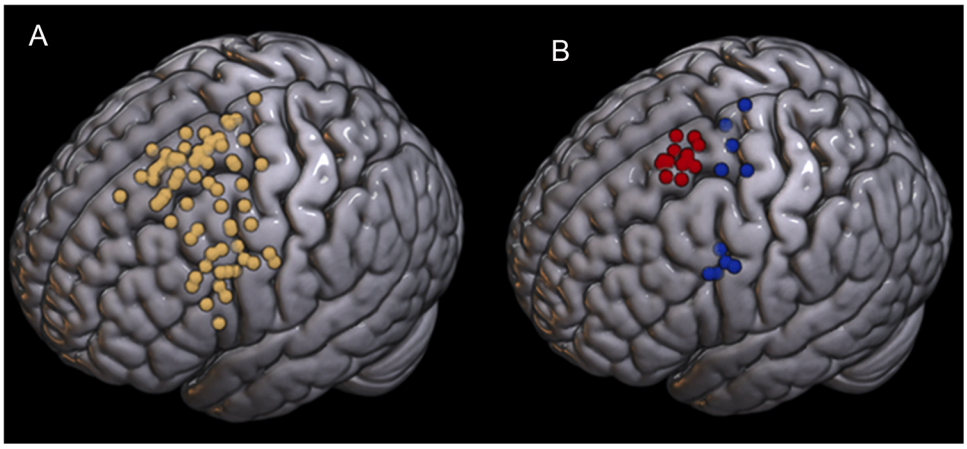

Fig. 3. Individual electrode positions are shown as a spherical volume (5 mm diameter) centred on the MNI coordinate corresponding to the actual electrode placement. All electrodes have been flipped on the left hemisphere to ensure comparability. A: cathodal electrode positions of all 14 strips on an MNI152 template render. B: positions of cathodal electrodes that showed effective conditioning on M1. Red electrodes indicate excitatory connectivity. Blue electrodes indicate inhibitory connectivity.

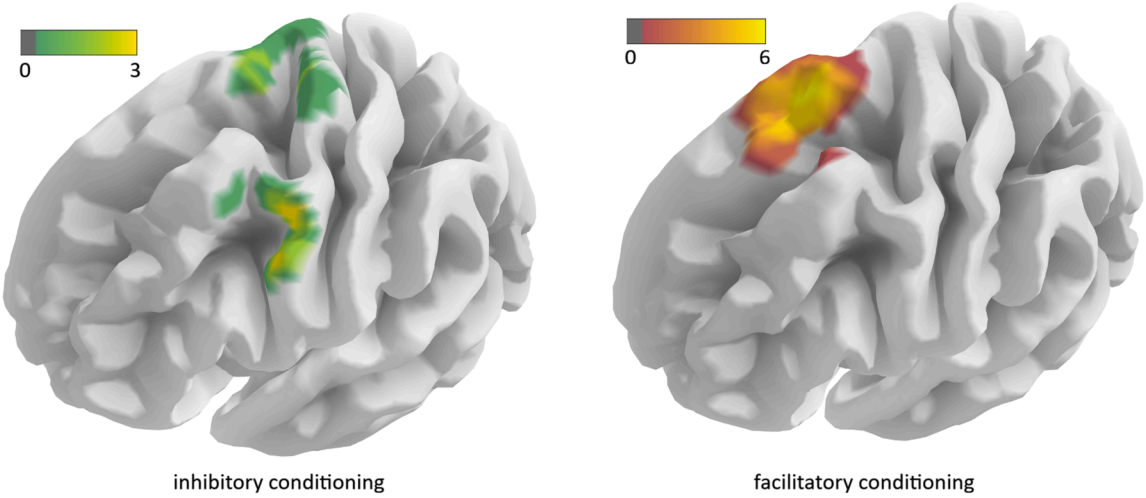

Fig. 4. Overlap density surface maps of the effective conditioning electrodes. the electrodes with inhibitory and with excitatory effects are represented separately.

4. Discussion

4.1. Summary of results

In the present work we investigate the short-latency functional connections between the premotor cortex and the ipsilateral upper limb representation in M1 in anesthetised adult humans with supratentorial brain tumours. The results highlight a converging network of superficial We found 3 distinct foci in the premotor cortex that give rise to short-latency effects on corticospinal excitability. Two inhibitory foci were localized along the precentral sulcus and one more rostrally, on the convexity of the superior frontal gyrus.

Table 2
individual coordinates of each stimulating strip electrode in MNI reference space. Electrodes with excitatory conditioning effects on M1 are marked in bold red font. Electrodes with inhibitory effects are marked in bold blue font.

Pat#	Coordinates in MNI space (x; y; z) of the Inter-electrodes point					
	P01	P02	P03	P04	P05	P06
#1	(14.5; −5.3; 77.2)	(14.5; 4.3; 74.3)	(14.5; 13.1; 69.8)	(14.5; 22.7; 65.4)	(13.8; 31.6; 61)	(13.8; 41.2; 55.1)
#2	(10.9; −19.3; 80.9)	(15.2; −9; 77.2)	(19.7; 0.6; 74.2)	(22.7; 10.9; 71.3)	(24.1; 20.5; 66.1)	(25.6; 27.1; 59.5)
#3	(−36.7; −9.7; 69.8)	(−30.8; −0.9; 68.3)	(−25.6; 8.7; 69.1)	(−19; 17.5; 69.1)	(−14.5; 24.9; 63.9)	-
#4	(−24.1; −8.3; 73.5)	(−23.4; 1.3; 73.5)	(−21.2; 10.2; 72)	(−17.5; 19; 69)	(−14.5; 26.4; 63.2)	-
#5	(6.4; 23.5; 66.9)	(17.5; 19.8; 67.6)	(27.8; 15.3; 66.1)	(37.4; 10.2; 64.7)	-	-
#6	(−16.8; 27.9; 61)	(−27.1; 29.4; 58.8)	(−35.2; 29.4; 53.6)	(−44.1; 24.9; 49.9)	(−51.4; 19; 45.5)	-
#7	(9.4; 10.2; 72.8)	(21.2; 6.5; 72)	(30; −0.1; 69.8)	(38.9; −0.1; 64.7)	-	-
#8	(−16.8; −5.3; 77.2)	(−19; 4.3; 73.5)	(−23.4; 13.1; 69.8)	(−24.9; 22.7; 63.2)	(−27.1; 31.6; 57.3)	-
#9	(13.1; 20.5; 68.4)	(24.1; 21.2; 64.7)	(34.5; 22; 59.5)	(42.6; 21.2; 52.1)	(50.7; 19; 44.8)	-
#10	(−33; 11.7; 65.4)	(−42.6; 10.9; 60.2)	(−48.5; 9.4; 52.1)	-	-	-
#11	(−51.4; 2; 54.3)	(−51.4; 8; 45.5)	(−55.9; 14.6; 38.1)	(−58.8; 16.8; 28.5)	(−60.3; 20.5; 17.5)	-
#12	(−45.5; 2.1; 59.5)	(−47.7; 9.4; 53.6)	(−52.1; 15.3; 47)	(−51.4; 22; 40.3)	(−52.9; 28.6; 33.7)	-
#13	(60.3; −1.6; 44.8)	(55.8; 7.2; 41.8)	(55.8; 17.6; 38.9)	(52.9; 27.1; 37.4)	-	-
#14	(−61.8; −3.1; 41.1)	(−59.5; 5; 41.8)	(−55.1; 10.9; 36.6)	(−55.85; 18.3; 32.2)	(−56.6; 24.2; 25.6)	-

4.2. Limitations

The specific timing of the interactions between the two pulses is blurred by the use of trains of stimuli. The use of the high frequency trains to stimulate the cortex is standard procedure in intraoperative stimulation and has been demonstrated to be more efficient than single-pulse stimulations in evoking a corticofugal volley (Bander et al., 2020; Szelényi et al., 2011; Taniguchi et al., 1993). It is a common observation in intraoperative mapping, that single pulses fail to evoke MEPs. The consequence for the present data is uncertainty in terms of timing. While we know, by means of the latency of the MEP that the effective pulse in the test stimulus is the last one in the train, we do not know whether there are build-up effects during the train in both the conditioning and the test stimuli, making the information on timing less precise, with a potential noise in the order of milliseconds (i.e. the duration of the train itself). While the spatial sampling of the premotor cortex by means of conditioning stimulation was appropriately dense (Fig. 3A), it should be taken into consideration that direct cortical stimulation procedures have a strong spatial bias towards the crown of the cortical gyri, since it is not common clinical practice to open the sulci. Therefore, stimulation is limited to the convexity of the gyri and ignores any cortical representation in the banks of the sulci. A further limitation comes from the fact that we tested patients during general anaesthesia and therefore very little conjectures can be made on the function of the connectivity highlighted here, nor on the polarity (inhibition vs. excitation) of the connections. TIVA significantly modulates synaptic transmission, primarily by enhancing inhibitory gamma-aminobutyric acid type A (GABA-A) receptor activity and decreasing excitatory neurotransmission, leading to a functional suppression of neuronal activity, particularly in the cortex. Despite these effects, neurophysiological recordings, such as Motor Evoked Potentials (MEPs) and Somatosensory Evoked Potentials (SSEPs), remain fully feasible (Banoub et al., 2003; Hasan et al., 2018) because TIVA-based regimes cause less dose-dependent signal depression in cortical synapses compared to volatile anaesthetic agents and propofol's rapid metabolism allows for quick titration of the anaesthetic depth, minimizing synaptic depression. However conservative, TIVA still represents a limitation of synaptic transmission compared to the awake patient and therefore the quantity and polarity of the neurophysiological effects observed here. Further limitations include the fact that we did not explore different stimulation intensities cortico-cortical connections may be intensity-dependent, as for example it has been observed that low intensity CStims over PMv elicit excitatory effects on M1 and higher-intensity stimuli elicit inhibitory effects on M1 (Bäumer et al., 2009a). In addition, CStim effects are also task-dependent and can even reverse their polarity in the awake subject (Perez and Cohen, 2009). Summing up, we should resist the temptation to over-interpret neurophysiological evidence of inhibitory or facilitatory connections as evidence of behavioural inhibition or facilitation. We will discuss the results in comparison with previous data on ipsilateral, intrahemispheric premotor-M1 connectivity in humans. Though some works have explored crossed, interhemispheric premotor-M1 connections, the nature of such networks is beyond the interest of the current work. Finally, a possible caveat in the interpretation of the present data is the potential tumour-related disconnection, that may alter positive results or even produce false negative results. In light of this objection, the present data should be considered valid only in terms of positive findings, and taken cautiously when reporting absence of evidence, given the fact that the underlying brain circuits are likely to be not normally functioning.

4.3. Ventral and dorsal clusters in the precentral sulcus

We found two distinct regions along the precentral sulcus, corresponding to the conventional distinctions in ventral and dorsal premotor cortices (Gallivan and Culham, 2015). As expected from current models of the primate cortical motor system, both the PMv and the PMd show direct connectivity to the ipsilateral M1 (Dum and Strick, 2005; Shimazu et al., 2004). We found the precentral sulcus spots to be clustered in a ventral region and in a dorsal one. The ventral region corresponded roughly to the region dorsal to the junction between the inferior frontal sulcus and the precentral sulcus (Inferior Frontal Junction – IFJ). This locus compares favourably with the ventral precentral cluster observed in the whole-hemisphere investigation by Cattaneoand Barchiesi (2011). Other dual coil TMS studies in humans investigating the ventral precentral region, all found short latency effects during rest (Bäumer et al., 2009b; Cattaneo and Barchiesi, 2011; Groppa et al., 2012; Shields et al., 2016), during visually-guided grasping (Davare et al., 2009, 2008; Maule et al., 2015), action observation (Koch et al., 2010; Lago et al., 2010) and intransitive movements (Houdayer et al., 2012). In comparison with previous intraoperative DCS studies, our mean coordinates of x=−51.8, y = 2.0, z =45.3 are marginally external to the ventral premotor corticospinal fields described by Fornia et al. (2018) and have a good correspondence with the cortical regions that evoke a clumsy manipulation behaviour shown in Fornia et al. (2020).It is worth noting that all patients in the current series showed that the origin of PMv-M1 connections is localized dorsally to the IFJ, suggesting that the human PMv region that controls hand movements may be completely localized above the inferior frontal sulcus. In terms of timing of the connections, the CStim-TStim interactions previously observed with TMS range in the

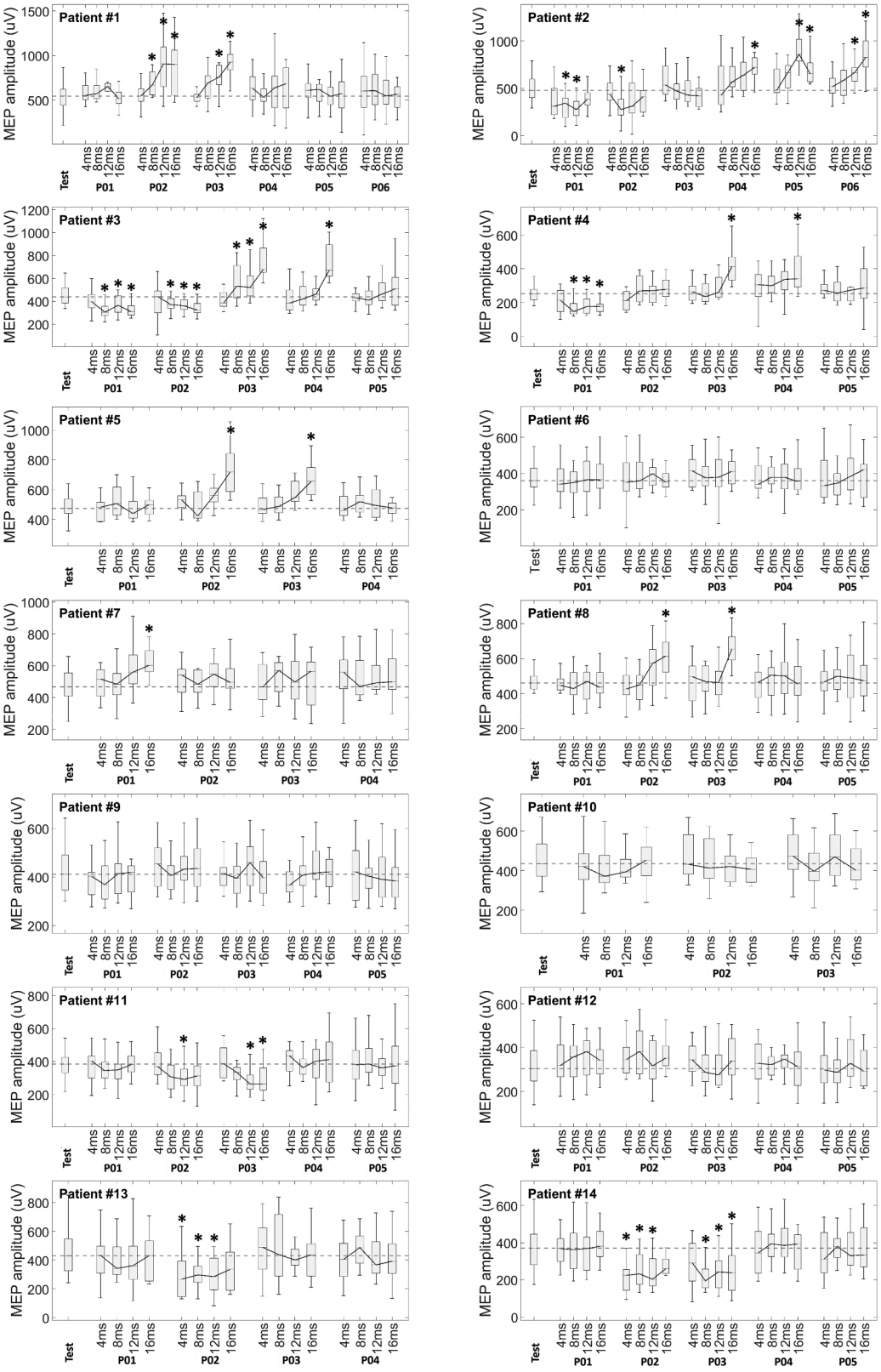

Fig. 5. Boxplot of the MEP amplitudes in individual patients and in all the different experimental conditions. The boxes indicates median, 1st and 3rd quartile. The whiskers represent the extreme values. The data relative to MEPs to TestStim alone (Test) and to CStim+TStim. The # indicates the patient's unique identifier and the dashed horizontal line indicates the TestStim MEP median amplitude, to be considered as baseline condition, to which the conditioned MEPs are to be compared. ISIs from 4 to 16 ms are indicated. Asterisks indicate conditions with MEPs that are significantly distributed differently from the baseline (*t*-test for paired samples with Bonferroni-Holmes correction). All the numerical values and statistical parameters at the origin of the illustration are reported in Supplementary Table 1.

4–7 ms range, similarly to the average latency observed in the present dataset, confirming the hypothesis of a direct or quasi-direct cortico--cortical route.

We observed a cluster of inhibitory active spots along a dorsal portion of the precentral sulcus, which may correspond to a putative human PMd as commonly defined in functional and anatomical imaging studies (Cavina-Pratesi et al., 2018; Chouinard and Paus, 2006; Gallivan and Culham, 2015; Genon et al., 2018; Guye et al., 2003; Schubotz and Von Cramon, 2003; Tomassini et al., 2007) that investigate the topography of upper limb representations in the dorsal precentral complex. Concerning dual-coil TMS studies, the anatomical proximity of the precentral focus to the M1-hand representation makes it impossible for conventional dual-coil positioning (Hehl et al., 2024b), therefore no direct comparison can be made with most TMS studies. One study reportedly stimulated the precentral sulcus region with conditioning TMS and found reach and grasp-related excitation of the hand motor cortex (Vesia et al., 2018). Further suggestions on the functional identity of the dPreCS cluster is that it overlaps with the cortical region that was identified in a study investigating the lesional volumes in human brains associated with clinical deficit in visually-guided object grasping. (Di Caro et al., 2025). The results of the Neurosynth (Yarkoni et al., 2011) meta-analyisis of previous imaging studies on "grasping", compared to the current results (Fig. 5), showed a substantial overlap between the dorsal premotor and ventral premotor fMRI activity and our dPreCS and vPreCS foci. Taken together the data from dual coil TMS and the functional imaging meta-analytical data, knowledge suggests that the two precentral foci, dorsal and ventral, are very likely subserving hand control for sensory-guided manipulation, through direct corticocortical connections. They probably correspond to the dorsal and ventral PM regions in humans (Rizzolatti et al., 2014).

4.4. The superior frontal gyrus cluster

We observed a cluster of active electrode positions in the convexity of the superior frontal gyrus that appeared to be clearly distinct from the more posterior dPreCS cluster both anatomically, being located some 2.5 cm anteriorly, and functionally, being excitatory rather than inhibitory. This separate dorsal cluster is located 4- 5 cm from the central sulcus, therefore making it a good putative candidate for the cortical region that has been stimulated with conditioning TMS in most dual-coil studies, where the physical interactions between the two coils allowed only for stimulation of a more anterior region (Bäumer et al., 2009b; Byblow et al., 2007; Civardi et al., 2001; Hoornweder et al., 2021) or where the specific anterior SFG regions were targeted ad-hoc (Cattaneo and Parmigiani, 2021; Parmigiani et al., 2018, 2015). The few experiments where such connectivity was tested in task-related settings shows that the pattern of motor commands that are transferred to M1 seem more complex than simple visuomotor association that are instead found in the more caudal dPreCS focus (cfr. Vesia et al., 2018). Indeed (Parmigiani et al., 2018) found that the SFG-M1 connections contained information on inhibitory set-related activity during action preparation in a delayed reaction task with a predictable timing of the GO-signal. (Byblow et al., 2007) found that the SFG-M1 connectivity was involved in coordination of movement phases of whole-body actions. It is challenging to identify a clear role of the SFG-M1 connections that are described here. The caudal convexity of the SFG is supposedly involved in action strategies that involve internal timing (Brancaccio et al., 2025; Tagliaferri et al., 2023, 2024b). We can hypothesize that the SFG-M1 connections perform contingent, task phase-dependent control over hand actions but testing in awake patients will be needed to confirm this. The finding of a short-latency effect of SFG stimulation on the ipsilateral M1 possibly sheds some new light on non-invasive stimulation studies that targeted the supplementary motor area (SMA)-M1 circuitry (Arai et al., 2012, 2011). Indeed, targeting TMS of the supplementary motor region involves necessarily stimulation of the more superficial SFG cortex. Therefore, it is possible that established SMA-M1 network effects dould be due at least in part to a mixture of SMA/SFG stimulation effects.

4.5. Timing of the premotor-motor interactions

The present study has some limitations in identifying precise timing of the PM-M1 interactions. Both CondStim and TestStim were delivered in short trains of 3 stimuli, 4.6 ms in duration, which are too long to be considered as single time points. The temporal resolution of the study is therefore sub-optimal. We calculated the ISI between the last stimulus of the CondStim train and the last stimulus of the TestStim train, assuming that it is the last train of the stimulus that gives off the corticofugal volley. This is a valid and currently accepted hypothesis for the TestStim over M1, but we are left with the uncertainty about the possible effects of the earlier pulses in the train. This said, we observed effective interactions from the premotor cortex to M1, ranging in the 4–12 ms interval, depending on the stimulated spot and on the individual. The earliest effective ISIs compare well with those from the dual-TMS literature (see Malderen et al. (2023)) for a review of effective ISIs in dual-coil TMS protocols). The dPreCS and vPreCS clusters had earliest effective ISIs of 4 ms, that are fully compatible with a direct cortico-cortical connection. The SFG cluster showed conditioning effects at the earliest ISI of 8 ms, which is both compatible with a direct cortico-cortical route, but also potentially compatible with an indirect pathway, either through another cortical relay or through the basal ganglia circuits. The SFG convexity region is indeed at the origin of fibers to the ventral premotor cortex, through the Frontal Aslant Tract (Tagliaferri et al., 2024b, 2024a, 2023) and of corticostriatal fibers, providing anatomical support of the indirect route hypothesis. Data on whole-brain effects of focal brain stimulation can be of help in hypothesizing potential networks through which the premotor-motor interactions occur and indeed support both the possibilities of a cortico-cortical and cortico-subcortical indirect route (Bestmann et al., 2008, 2005). The empirical information obtained in the present study does not allow us to disentangle any of the potential pathways. It is worth noting that the dual-electrode technique that we propose here has systematically yielded slightly longer latencies than the dual coil TMS counterpart. For example Groppa et al. (2012) found PMd-M1 interactions at ISIs around 2 ms compared to our current results of 4.6 ms. Similarly, in our previous work on dual-site cortical stimulation of the parietal-M1 circuits (Cattaneo et al., 2020) we found minimum ISIs (4 ms) that were slightly longer that the shortest ISIs reported in the TMS literature, i.e. 2 ms (Karabanov et al., 2013). Along the same line, using direct cortical stimulation we demonstrated cerebellar cortical inhibition with a minimum latency of 8 ms (Giampiccolo et al., 2021), compared to the minimum ISI of 4 ms observed with TMS (Ugawa et al., 1995). This discrepancy is at least in part due to the fact that due to the use of trains of 3 stimuli, 4.6 ms was the minimum ISI in the protocol, but is probably also due to the fact that TMS at the intensities used in the literature stimulates a larger and deeper volume of brain tissue. Finally, the PMd has been recently described as forming a structural-functional continuum with M1-hand in the precentral hand knob, and that local myelin content predicts neurophysiological and behavioral individual characteristics (Dubbioso et al., 2021). This previous finding indicates that inter-individual structural variability may be significantly high to justify inter-individual variability in the timing of the PM-M1 interactions, therefore reflecting pre-existing structural variability rather than only synaptic connectivity.

4.6. Possible functional role of premotor-motor circuitry and implications for intraoperative neurophysiological monitoring

The current data are based on anesthetized patients and therefore any inference on the behavioural role of our findings can only be speculative. However, some inference can be done based on topography of the premotor hotspots and on the fact that we assessed corticospinal

function controlling the distal upper limb. The two precentral sulcus clusters are likely to be homologous of the ventral and dorsal premotor cortices (PMv and PMd) and therefore are probably related to visuo-motor transformations for visually-guided hand-object interactions (Cattaneo et al., 2005; Di Caro et al., 2025; Shimazu et al., 2004). Less clear is the putative function of the SFG region, though topographical analogy with other studies (Cattaneo and Parmigiani, 2021; Parmigiani and Cattaneo, 2018) seem to indicate a role in executive control over action timing. A clinical investigation on the role of the circuitry in behavior is a necessary step towards a possible application of the paired stimulation technique in routine intraoperative monitoring. Intra-operative neurophysiology is increasingly used in Neurosurgery to preserve brain functions while maximizing tumour resection. Cortical MEPs are the gold standard for monitoring the cortico-spinal tract but these cannot assess the integrity of higher motor function circuits, which are typically assess during awake surgery to allow for neuropsychological testing. In the recent past, cortico-cortical evoked potentials (CCEPs) have been increasingly used to monitor the arcuate fascicle under general anesthesia, opening to the possibility to monitor the functional integrity of language or other cognitive pathways also in patients who are poor candidates for an awake craniotomy. In this perspective, the conditioned-test stimuli paradigm that we used in the current and previous studies (Cattaneo et al., 2020; Giampiccolo et al., 2021; Sala et al., 2021) sheds a new light on the possibility to expand intraoperative neurophysiological monitoring to assess brain connectivity during neurosurgical procedures, under general anaesthesia. The preservation throughout surgery of a baseline, inhibitory or facilitatory effect, would imply the preservation of the underlying connectivity while, vice versa, a iatrogenic injury to this connectivity should result in the loss of the modulatory effect. Yet, future studies are needed for the standardization of the technique and, above all, the correlation with the clinical outcome. This latter may be challenging to evaluate given the uncertainties related to the function underlying some of these circuits and the related neurological deficits.

Data and code availability statements

No specific code has been used to analyze the data.

The data are available upon request in anonymised and derivative form. Raw clinical data or any datum that can result in identification of the patient are not available.

CRediT authorship contribution statement

Luigi Cattaneo: Writing – review & editing, Writing – original draft, Visualization, Validation, Supervision, Methodology, Investigation, Funding acquisition, Formal analysis, Data curation, Conceptualization. **Sonia Nunes:** Writing – review & editing, Writing – original draft, Visualization, Validation, Methodology, Investigation, Data curation. **Davide Giampiccolo:** Writing – review & editing, Writing – original draft, Validation, Supervision, Methodology, Data curation, Conceptualization. **Valeria Di Caro:** Writing – review & editing, Writing – original draft, Validation, Resources, Methodology, Investigation, Formal analysis. **Federica Basaldella:** Writing – review & editing, Visualization, Validation, Methodology, Investigation, Formal analysis. **Andrea Badari:** Writing – review & editing, Visualization, Validation, Methodology, Investigation, Formal analysis. **Marco Tagliaferri:** Writing – review & editing, Visualization, Validation, Methodology, Formal analysis. **Giovanna Squintani:** Writing – review & editing, Visualization, Validation, Supervision, Methodology, Investigation, Conceptualization. **Francesco Sala:** Writing – review & editing, Writing – original draft, Visualization, Validation, Supervision, Resources, Project administration, Methodology, Investigation, Funding acquisition, Conceptualization.

Declaration of competing interest

None of the authors report any conflict of interest

Acknowledgments

This work was supported by the CaRiVerona foundation for the project “Neuro-Connect - Systems neuroscience meets clinical neurosurgery: development of novel multimodal monitoring indices of brain connectivity in patients with glioma” ID ROL10768 COD.SIME 2018.0911, and by the European Union – Next Generation EU- PRIN 2022 PNRR (DD 1409 del 14/09/22) – PNRR – M4 – C2 – INV1.1 – PRIN –Project title "Motivated behaviour in the medial premotor areas, in health and disease" – codice identificativo progetto 2022F7ZRS3 – CUP (University of Trento) E53D2302215 0006 - fondo [40104637 - CATTANEO PRIN 2022] – CUP (University of Verona) B53D23033870006 - fondo [SALA_PRIN2022]. DG is supported by the Epilepsy Research Institute UK with an Emerging Leaders fellowship (grant F2403).

Supplementary materials

Supplementary material associated with this article can be found, in the online version, at doi:10.1016/j.neuroimage.2025.121621.

References

Amunts, K., Mohlberg, H., Bludau, S., Zilles, K., 2020. Julich-Brain: a 3D probabilistic atlas of the human brain’s cytoarchitecture. Science 369, 988–992. https://doi.org/10.1126/science.abb4588.

Arai, N., Lu, M.K., Ugawa, Y., Ziemann, U., 2012. Effective connectivity between human supplementary motor area and primary motor cortex: a paired-coil TMS study. Exp. Brain Res. 220, 79–87. https://doi.org/10.1007/s00221-012-3117-5.

Arai, N., Müller-Dahlhaus, F., Murakami, T., Bliem, B., Lu, M.-K., Ugawa, Y., Ziemann, U., 2011. State-dependent and timing-dependent bidirectional associative plasticity in the human SMA-M1 network. J. Neurosci. 31, 15376–15383. https://doi.org/10.1523/JNEUROSCI.2271-11.2011.

Bander, E.D., Shelkov, E., Modik, O., Kandula, P., Karceski, S.C., Ramakrishna, R., 2020. Use of the train-of-five bipolar technique to provide reliable, spatially accurate motor cortex identification in asleep patients. Neurosurg. Focus. 48, E4. https://doi.org/10.3171/2019.11.FOCUS19776.

Banoub, M., Tetzlaff, J.E., Schubert, A., 2003. Pharmacologic and physiologic influences affecting sensory evoked potentials: implications for perioperative monitoring. Anesthesiology 99, 716–737. https://doi.org/10.1097/00000542-200309000-00029.

Bäumer, T., Schippling, S., Kroeger, J., Zittel, S., Koch, G., Thomalla, G., Rothwell, J.C., Siebner, H.R., Orth, M., Münchau, A., 2009a. Inhibitory and facilitatory connectivity from ventral premotor to primary motor cortex in healthy humans at rest – a bifocal TMS study. Clin. Neurophysiol. 120, 1724–1731. https://doi.org/10.1016/J.CLINPH.2009.07.035.

Bäumer, T., Schippling, S., Kroeger, J., Zittel, S., Koch, G., Thomalla, G., Rothwell, J.C., Siebner, H.R., Orth, M., Münchau, A., 2009b. Inhibitory and facilitatory connectivity from ventral premotor to primary motor cortex in healthy humans at rest–a bifocal TMS study. Clin. Neurophysiol. 120, 1724–1731. https://doi.org/10.1016/j.clinph.2009.07.035.

Bestmann, S., Baudewig, J., Siebner, H.R., Rothwell, J.C., Frahm, J., 2005. BOLD MRI responses to repetitive TMS over human dorsal premotor cortex. Neuroimage 28, 22–29. https://doi.org/10.1016/j.neuroimage.2005.05.027.

Bestmann, S., Swayne, O., Blankenburg, F., Ruff, C.C., Haggard, P., Weiskopf, N., Josephs, O., Driver, J., Rothwell, J.C., Ward, N.S., 2008. Dorsal premotor cortex exerts state-dependent causal influences on activity in contralateral primary motor and dorsal premotor cortex. Cereb. Cortex. 18, 1281–1291. https://doi.org/10.1093/cercor/bhm159.

Borra, E., Belmalih, A., Gerbella, M., Rozzi, S., Luppino, G., 2010. Projections of the hand field of the macaque ventral premotor area F5 to the brainstem and spinal cord. J. Comp. Neurol. 518, 2570–2591. https://doi.org/10.1002/cne.22353.

Brancaccio, A., Tagliaferri, M., Miniussi, C., Cattaneo, L., 2025. Brain signatures of predictive and reactive strategies in a simple delayed reaction time task: an EEG study. NeuroImage Press.

Byblow, W.D., Coxon, J.P., Stinear, C.M., Fleming, M.K., Williams, G., Müller, J.F.M., Ziemann, U., 2007. Functional connectivity between secondary and primary motor areas underlying hand–Foot coordination. J. Neurophysiol. 98, 414–422. https://doi.org/10.1152/jn.00325.2007.

Caminiti, R., Innocenti, G.M., Battaglia-Mayer, A., 2015. Organization and evolution of parieto-frontal processing streams in macaque monkeys and humans. Neurosci. Biobehav. Rev. 56, 73–96. https://doi.org/10.1016/j.neubiorev.2015.06.014.

Casarotto, A., Dolfini, E., Cardellicchio, P., Fadiga, L., D’Ausilio, A., Koch, G., 2023. Mechanisms of Hebbian-like plasticity in the ventral premotor – primary motor network. J. Physiol. 601, 211–226. https://doi.org/10.1113/JP283560.

Casini, L., Vidal, F., 2011. The SMAs: Neural substrate of the temporal accumulator? Front. Integr. Neurosci. 5, 35. https://doi.org/10.3389/fnint.2011.00035.
Cattaneo, L., 2017. Transcranial magnetic stimulation. Eds.. In: Rogers, L., Vallortigara, G. (Eds.), Lateralized Brain Functions. Springer, Berlin Heidelberg, pp. 369–406.
Cattaneo, L., Barchiesi, G., 2011. Transcranial magnetic mapping of the short-latency modulations of corticospinal activity from the ipsilateral hemisphere during rest. Front. Neural Circuits. 5, 1–13. https://doi.org/10.3389/fncir.2011.00014.
Cattaneo, L., Giampiccolo, D., Meneghelli, P., Tramontano, V., Sala, F., 2020. Cortico-cortical connectivity between the superior and inferior parietal lobules and the motor cortex assessed by intraoperative dual cortical stimulation. Brain Stimul. 13, 819–831. https://doi.org/10.1016/J.BRS.2020.02.023.
Cattaneo, L., Parmigiani, S., 2021. Stimulation of different sectors of the Human dorsal premotor cortex induces a shift from reactive to predictive action strategies and changes in motor inhibition: a dense transcranial magnetic Stimulation (TMS) mapping study. Brain Sci. 11, 534. https://doi.org/10.3390/BRAINSCI11050534, 2021, Vol. 11, p. 534–534.
Cattaneo, L., Voss, M., Brochier, T., Prabhu, G., Wolpert, D.M., Lemon, R.N., 2005. A cortico-cortical mechanism mediating object-driven grasp in humans. In: Proceedings of the National Academy of Sciences of the United States of America, 102, pp. 898–903. https://doi.org/10.1073/pnas.0409182102.
Cavina-Pratesi, C., Connolly, J.D., Monaco, S., Figley, T.D., Milner, A.D., Schenk, T., Culham, J.C., 2018. Human neuroimaging reveals the subcomponents of grasping, reaching and pointing actions. Cortex 98, 128–148. https://doi.org/10.1016/j.cortex.2017.05.018.
Chouinard, P.A., Paus, T., 2006. The primary motor and premotor areas of the Human cerebral cortex. Neuroscientist 12, 143–152. https://doi.org/10.1177/1073858405284255.
Cisek, P., Kalaska, J.F., 2010. Neural mechanisms for interacting with a world full of action choices. Annu Rev. Neurosci. 33, 269–298. https://doi.org/10.1146/annurev.neuro.051508.135409.
Civardi, C., Cantello, R., Asselman, P., Rothwell, J.C., 2001. Transcranial magnetic stimulation can Be used to test connections to primary motor areas from frontal and medial cortex in humans. Neuroimage 14, 1444–1453. https://doi.org/10.1006/nimg.2001.0918.
Coull, J.T., Vidal, F., Burle, B., 2016. When to act, or not to act: that's the SMA's question. current opinion in behavioral sciences. Time Percept. Action 8, 14–21. https://doi.org/10.1016/j.cobeha.2016.01.003.
Davare, M., Lemon, R., Olivier, E., 2008. Selective modulation of interactions between ventral premotor cortex and primary motor cortex during precision grasping in humans. J. Physiol. 586, 2735–2742. https://doi.org/10.1113/jphysiol.2008.152603.
Davare, M., Montague, K., Olivier, E., Rothwell, J.C., Lemon, R.N., 2009. Ventral premotor to primary motor cortical interactions during object-driven grasp in humans. Cortex 45, 1050–1057. https://doi.org/10.1016/J.CORTEX.2009.02.011.
Di Caro, V., Cesari, P., Sala, F., Cattaneo, L., 2025. The neural bases of the reach–grasp movement in humans: quantitative evidence from brain lesions. Proc. Natl. Acad. Sci. 122, e2419801122. https://doi.org/10.1073/pnas.2419801122.
Di Luzio, P., Brady, L., Turrini, S., Romei, V., Avenanti, A., Sel, A., 2024. Investigating the effects of cortico-cortical paired associative stimulation in the human brain: a systematic review and meta-analysis. Neurosci. Biobehav. Rev. 167, 105933. https://doi.org/10.1016/j.neubiorev.2024.105933.
Dubbioso, R., Madsen, K.H., Thielscher, A., Siebner, H.R., 2021. The myelin content of the Human precentral hand knob reflects interindividual differences in manual motor control at the physiological and behavioral level. J. Neurosci. 41, 3163–3179. https://doi.org/10.1523/JNEUROSCI.0390-20.2021.
Dum, R.P., Strick, P.L., 2005. Frontal lobe inputs to the digit representations of the motor areas on the lateral surface of the hemisphere. J. Neurosci. 25, 1375–1386. https://doi.org/10.1523/JNEUROSCI.3902-04.2005.
Ferbert, A., Priori, A., Rothwell, J.C., Day, B.L., Colebatch, J.G., Marsden, C.D., 1992. Interhemispheric inhibition of the human motor cortex. J. Physiol. 453, 525–546. https://doi.org/10.1113/JPHYSIOL.1992.SP019243.
Fornia, L., Ferpozzi, V., Montagna, M., Rossi, M., Riva, M., Pessina, F., Boneschi, F.M., Borroni, P., Lemon, R.N., Bello, L., Cerri, G., 2018. Functional characterization of the left ventrolateral premotor cortex in humans: a direct electrophysiological approach. Cereb. Cortex. 28, 167–183. https://doi.org/10.1093/cercor/bhw365.
Fornia, L., Rossi, M., Rabuffetti, M., Leonetti, A., Puglisi, G., Viganò, L., Simone, L., Howells, H., Bellacicca, A., Bello, L., Cerri, G., 2020. Direct electrical stimulation of premotor areas: different effects on hand muscle activity during object manipulation. Cereb. Cortex. 30, 391–405. https://doi.org/10.1093/cercor/bhz139.
Gallivan, J.P., Culham, J.C., 2015. Neural coding within human brain areas involved in actions. Curr. Opin. Neurobiol. 33, 141–149. https://doi.org/10.1016/j.conb.2015.03.012.
Genon, S., Reid, A.T., Li, H., Fan, L., Muller, V., Cieslik, E.C., Hoffstaedter, F., Langner, R., Grefkes, C., Laird, A.R., Fox, P.T., Jiang, T., Amunts, K., Eickhoff, S.B., 2018. The heterogeneity of the left dorsal premotor cortex evidenced by multimodal connectivity-based parcellation and functional characterization. Neuroimage 170, 400–411. https://doi.org/10.1016/J.NEUROIMAGE.2017.02.034.
Giampiccolo, D., Basaldella, F., Badari, A., Squintani, G.M., Cattaneo, L., Sala, F., 2021. Feasibility of cerebello-cortical stimulation for intraoperative neurophysiological monitoring of cerebellar mutism. Child's Nerv. Syst. 37, 1505–1514. https://doi.org/10.1007/S00381-021-05126-7/FIGURES/6.
Giampiccolo, D., Nunes, S., Cattaneo, L., Sala, F., 2022. Functional approaches to the surgery of brain gliomas. Ed.. In: Di Rocco, C. (Ed.), Advances and Technical Standards in Neurosurgery, Advances and Technical Standards in Neurosurgery, 45. Springer International Publishing, Cham, pp. 35–96. https://doi.org/10.1007/978-3-030-99166-1_2.
Graziano, M.S.A., 2016. Ethological action maps: a paradigm shift for the motor cortex. Trends. Cogn. Sci. 20, 121–132. https://doi.org/10.1016/j.tics.2015.10.008.
Groppa, S., Werner-Petroll, N., Münchau, A., Deuschl, G., Ruschworth, M.F.S., Siebner, H.R., 2012. A novel dual-site transcranial magnetic stimulation paradigm to probe fast facilitatory inputs from ipsilateral dorsal premotor cortex to primary motor cortex. Neuroimage 62, 500–509. https://doi.org/10.1016/j.neuroimage.2012.05.023.
Guye, M., Parker, G.J.M., Symms, M., Boulby, P., Wheeler-Kingshott, C.A.M., Salek-Haddadi, A., Barker, G.J., Duncan, J.S., 2003. Combined functional MRI and tractography to demonstrate the connectivity of the human primary motor cortex in vivo. Neuroimage 19, 1349–1360. https://doi.org/10.1016/S1053-8119(03)00165-4.
Hanajima, R., Ashby, P., Lang, A.E., Lozano, A.M., 2002. Effects of acute stimulation through contacts placed on the motor cortex for chronic stimulation. Clin. Neurophysiol. 113, 635–641. https://doi.org/10.1016/S1388-2457(02)00042-1.
Hasan, M.S., Tan, J.K., Chan, C.Y.W., Kwan, M.K., Karim, F.S.A., Goh, K.J., 2018. Comparison between effect of desflurane/remifentanil and propofol/remifentanil anesthesia on somatosensory evoked potential monitoring during scoliosis surgery—a randomized controlled trial. J. Orthop. Surg. 26, 2309499018789529. https://doi.org/10.1177/2309499018789529.
Hehl, M., Van Malderen, S., Geraerts, M., Meesen, R.L.J., Rothwell, J.C., Swinnen, S.P., Cuypers, K., 2024a. Probing intrahemispheric interactions with a novel dual-site TMS setup. Clin. Neurophysiol. 158, 180–195. https://doi.org/10.1016/j.clinph.2023.12.128.
Hehl, M., Van Malderen, S., Geraerts, M., Meesen, R.L.J., Rothwell, J.C., Swinnen, S.P., Cuypers, K., 2024b. Probing intrahemispheric interactions with a novel dual-site TMS setup. Clin. Neurophysiol. 158, 180–195. https://doi.org/10.1016/j.clinph.2023.12.128.
Hoornweder, S.V., Debeuf, R., Verstraelen, S., Meesen, R., Cuypers, K., 2021. Unravelling ipsilateral interactions between left dorsal premotor and primary motor cortex: a proof of concept study. Neuroscience 466, 36–46. https://doi.org/10.1016/j.neuroscience.2021.04.033.
Houdayer, E., Beck, S., Karabanov, A., Poston, B., Hallett, M., 2012. The differential modulation of the ventral premotor–motor interaction during movement initiation is deficient in patients with focal hand dystonia. Eur. J. Neurosci. 35, 478–485. https://doi.org/10.1111/j.1460-9568.2011.07960.x.
Iles, J.F., 2005. Simple models of stimulation of neurones in the brain by electric fields. Prog. Biophys. Mol. Biol. 87, 17–31. https://doi.org/10.1016/j.pbiomolbio.2004.06.002.
Isa, T., Kinoshita, M., Nishimura, Y., 2013. Role of direct vs. indirect pathways from the motor cortex to spinal motoneurons in the control of hand dexterity. Front. Neurol. 4. https://doi.org/10.3389/fneur.2013.00191.
Karabanov, A.N., Chao, C.C., Paine, R., Hallett, M., 2013. Mapping different intra-hemispheric parietal-motor networks using Twin coil TMS. Brain Stimul. 6, 384–389. https://doi.org/10.1016/j.brs.2012.08.002.
Koch, G., 2020. Cortico-cortical connectivity: the road from basic neurophysiological interactions to therapeutic applications. Exp. Brain Res. https://doi.org/10.1007/s00221-020-05844-5.
Koch, G., Rothwell, J.C., 2009. TMS investigations into the task-dependent functional interplay between human posterior parietal and motor cortex. Behav. Brain Res. 202, 147–152. https://doi.org/10.1016/J.BBR.2009.03.023.
Koch, G., Versace, V., Bonnì, S., Lupo, F., Lo Gerfo, E., Oliveri, M., Caltagirone, C., 2010. Resonance of cortico-cortical connections of the motor system with the observation of goal directed grasping movements. Neuropsychologia 48, 3513–3520. https://doi.org/10.1016/j.neuropsychologia.2010.07.037.
Lafleur, L.P., Tremblay, S., Whittingstall, K., Lepage, J.F., 2016. Assessment of effective connectivity and plasticity with dual-coil transcranial magnetic stimulation. Brain Stimul. 9, 347–355. https://doi.org/10.1016/J.BRS.2016.02.010.
Lago, A., Koch, G., Cheeran, B., Márquez, G., Sánchez, J.A., Ezquerro, M., Giraldez, M., Fernández-del-Olmo, M., 2010. Ventral premotor to primary motor cortical interactions during noxious and naturalistic action observation. Neuropsychologia 48, 1802–1806. https://doi.org/10.1016/j.neuropsychologia.2010.02.030.
Lemon, R., 2019. Recent advances in our understanding of the primate corticospinal system. https://doi.org/10.12688/f1000research.17445.1.
Lemon, R.N., 2008. Descending pathways in motor control. Annu. Rev. Neurosci. 31, 195–218. https://doi.org/10.1146/annurev.neuro.31.060407.125547.
Malderen, S.V., Hehl, M., Verstraelen, S., Swinnen, S.P., Cuypers, K., 2023. Dual-site TMS as a tool to probe effective interactions within the motor network: a review. Rev. Neurosci. 34, 129–221. https://doi.org/10.1515/revneuro-2022-0020.
Manola, L., Holsheimer, J., Veltink, P., Buitenweg, J.R., 2007. Anodal vs cathodal stimulation of motor cortex: a modeling study. Clin. Neurophysiol. 118, 464–474. https://doi.org/10.1016/j.clinph.2006.09.012.
Maule, F., Barchiesi, G., Brochier, T., Cattaneo, L., 2015. Haptic working memory for grasping: the role of the parietal operculum. Cereb. Cortex. 25, 528–537. https://doi.org/10.1093/cercor/bht252.
Parmigiani, S., Barchiesi, G., Cattaneo, L., 2015. The dorsal premotor cortex exerts a powerful and specific inhibitory effect on the ipsilateral corticofacial system: a dual-coil transcranial magnetic stimulation study. Exp. Brain Res. 233, 3253–3260. https://doi.org/10.1007/s00221-015-4393-7.
Parmigiani, S., Cattaneo, L., 2018. Stimulation of the dorsal premotor cortex, but not of the supplementary motor area proper, impairs the stop function in a STOP signal task. Neuroscience 394, 14–22. https://doi.org/10.1016/j.neuroscience.2018.10.005.

Parmigiani, S., Zattera, B., Barchiesi, G., Cattaneo, L., 2018. Spatial and temporal characteristics of set-related inhibitory and excitatory inputs from the dorsal premotor cortex to the ipsilateral motor cortex assessed by dual-coil transcranial magnetic stimulation. Brain Topogr. https://doi.org/10.1007/s10548-018-0635-x.

Perez, M.A., Cohen, L.G., 2009. Interhemispheric inhibition between primary motor cortices: what have we learned? J. Physiol. 587, 725. https://doi.org/10.1113/JPHYSIOL.2008.166926. –725.

Pötter-Nerger, M., Fischer, S., Mastroeni, C., Groppa, S., Deuschl, G., Volkmann, J., Quartarone, A., Münchau, A., Siebner, H.R., 2009. Inducing homeostatic-like plasticity in human motor cortex through converging corticocortical inputs. J. Neurophysiol. 102, 3180–3190. https://doi.org/10.1152/jn.91046.2008.

Rizzolatti, G., Cattaneo, L., Fabbri-Destro, M., Rozzi, S., 2014. Cortical mechanisms underlying the organization of goal-directed actions and mirror neuron-based action understanding. Physiol. Rev. 94, 655–706. https://doi.org/10.1152/physrev.00009.2013.

Rizzolatti, G., Luppino, G., 2001. The cortical motor system. Neuron 31, 889–901. https://doi.org/10.1016/S0896-6273(01)00423-8.

Sala, F., Giampiccolo, D., Cattaneo, L., 2021. Novel asleep techniques for intraoperative assessment of brain connectivity. Front. Neurol. 12, 1021. https://doi.org/10.3389/FNEUR.2021.687030/BIBTEX. –1021.

Schubotz, R.I., Von Cramon, D.Y., 2003. Functional-anatomical concepts of human premotor cortex: evidence from fMRI and PET studies. Neuroimage 20, 120–131. https://doi.org/10.1016/j.neuroimage.2003.09.014.

Shields, J., Park, J.E., Srivanitchapoom, P., Paine, R., Thirugnanasambandam, N., Kukke, S.N., Hallett, M., 2016. Probing the interaction of the ipsilateral posterior parietal cortex with the premotor cortex using a novel transcranial magnetic stimulation technique. Clin. Neurophysiol. 127, 1475–1480. https://doi.org/10.1016/j.clinph.2015.06.031.

Shimazu, H., Maier, M.A., Cerri, G., Kirkwood, P.A., Lemon, R.N., 2004. Macaque ventral premotor cortex exerts powerful facilitation of motor cortex outputs to upper limb motoneurons. J. Neurosci. 24, 1200–1211. https://doi.org/10.1523/JNEUROSCI.4731-03.2004.

Szelényi, A., Senft, C., Jardan, M., Forster, M.T., Franz, K., Seifert, V., Vatter, H., 2011. Intra-operative subcortical electrical stimulation: a comparison of two methods. Clin. Neurophysiol. 122, 1470–1475. https://doi.org/10.1016/j.clinph.2010.12.055.

Tagliaferri, M., Amorosino, G., Voltolini, L., Giampiccolo, D., Avesani, P., Cattaneo, L., 2024a. A revision of the dorsal origin of the frontal aslant tract (FAT) in the superior frontal gyrus: a DWI-tractographic study. Brain Struct. Funct. 229, 987–999. https://doi.org/10.1007/s00429-024-02778-4.

Tagliaferri, M., Giampiccolo, D., Parmigiani, S., Avesani, P., Cattaneo, L., 2023. Connectivity by the frontal aslant tract (FAT) explains local functional specialization of the superior and inferior frontal gyri in humans when choosing predictive over reactive strategies: a tractography-guided TMS study. J. Neurosci. 43, 6920–6929. https://doi.org/10.1523/JNEUROSCI.0406-23.2023.

Tagliaferri, M., Glaubig, L., DiChiaro, V., Cattaneo, L., 2024b. Stimulation of the frontal aslant tract's origin in the caudal superior frontal gyrus alters ongoing spontaneous rhythmic activity independently from the effector. Evid. Tractogr. Guid. Transcranial Magn. Stimul. https://doi.org/10.1101/2024.11.21.624661.

Taniguchi, M., Cedzich, C., Taniguchi, M., Cedzich, C., Schramm, J., 1993. Modification of cortical stimulation for motor evoked potentials under general anesthesia: technical description. Neurosurgery 32, 219.

Tomassini, V., Jbabdi, S., Klein, J.C., Behrens, T.E.J., Pozzilli, C., Matthews, P.M., Rushworth, M.F.S., Johansen-Berg, H., 2007. Diffusion-weighted imaging tractography-based parcellation of the human lateral premotor cortex identifies dorsal and ventral subregions with anatomical and functional specializations. J. Neurosci. 27, 10259–10269. https://doi.org/10.1523/JNEUROSCI.2144-07.2007.

Ugawa, Y., Uesaka, Y., Terao, Y., Hanajima, R., Kanazawa, I., 1995. Magnetic stimulation over the cerebellum in humans. Ann. Neurol. 37, 703–713. https://doi.org/10.1002/ANA.410370603.

Vesia, M., Culham, J.C., Jegatheeswaran, G., Isayama, R., Le, A., Davare, M., Chen, R., 2018. Functional interaction between human dorsal premotor cortex and the ipsilateral primary motor cortex for grasp plans: a dual-site TMS study. Neuroreport 29, 1355–1359. https://doi.org/10.1097/WNR.0000000000001117.

Woolrich, M.W., Jbabdi, S., Patenaude, B., Chappell, M., Makni, S., Behrens, T., Beckmann, C., Jenkinson, M., Smith, S.M., 2009. Bayesian analysis of neuroimaging data in FSL. Neuroimage 45, S173–S186. https://doi.org/10.1016/j.neuroimage.2008.10.055.

World Medical Association, 2013. World Medical Association Declaration of Helsinki: ethical principles for medical research involving human subjects. JAMA 310, 2191–2194. https://doi.org/10.1001/jama.2013.281053.

Yamada, S., Enatsu, R., Kimura, Y., Komatsu, K., Akiyama, Y., Mikami, T., Ochi, S., Mikuni, N., 2021. Effects of polarity of bipolar sensorimotor direct cortical stimulation on intraoperative motor evoked potentials. Clin. Neurophysiol. 132, 2351–2356. https://doi.org/10.1016/j.clinph.2021.06.032.

Yarkoni, T., Poldrack, R.A., Nichols, T.E., Van Essen, D.C., Wager, T.D., 2011. Large-scale automated synthesis of human functional neuroimaging data. Nat. Methods 8, 665–670. https://doi.org/10.1038/nmeth.1635.

Yushkevich, P.A., Piven, J., Hazlett, H.C., Smith, R.G., Ho, S., Gee, J.C., Gerig, G., 2006. User-guided 3D active contour segmentation of anatomical structures: significantly improved efficiency and reliability. Neuroimage 31, 1116–1128. https://doi.org/10.1016/j.neuroimage.2006.01.015.